Check out how Laminar Wash systems replace centrifugation completely in handling cells

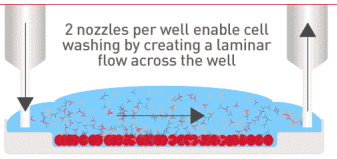

CURIOX
Accelerating Life Sciences
See How It Works

The Journal of Immunology

This information is current as of March 21, 2019.

Human Endothelial-Cell Specific Molecule-1 Binds Directly to the Integrin CD11a/CD18 (LFA-1) and Blocks Binding to Intercellular Adhesion Molecule-1

David Béchard, Arnaud Scherpereel, Hamida Hammad, Thibaut Gentina, Anne Tsicopoulos, Marc Aumercier, Jöel Pestel, Jean-Paul Dessaint, André-Bernard Tonnel and Philippe Lassalle

J Immunol 2001; 167:3099-3106; ;
doi: 10.4049/jimmunol.167.6.3099
http://www.jimmunol.org/content/167/6/3099

References This article **cites 37 articles**, 19 of which you can access for free at:
http://www.jimmunol.org/content/167/6/3099.full#ref-list-1

Why *The JI*? Submit online.

- **Rapid Reviews! 30 days*** from submission to initial decision
- **No Triage!** Every submission reviewed by practicing scientists
- **Fast Publication!** 4 weeks from acceptance to publication

**average*

Subscription Information about subscribing to *The Journal of Immunology* is online at:
http://jimmunol.org/subscription

Permissions Submit copyright permission requests at:
http://www.aai.org/About/Publications/JI/copyright.html

Email Alerts Receive free email-alerts when new articles cite this article. Sign up at:
http://jimmunol.org/alerts

The Journal of Immunology is published twice each month by
The American Association of Immunologists, Inc.,
1451 Rockville Pike, Suite 650, Rockville, MD 20852
Copyright © 2001 by The American Association of Immunologists All rights reserved.
Print ISSN: 0022-1767 Online ISSN: 1550-6606.

Downloaded from http://www.jimmunol.org/ by guest on March 21, 2019

Human Endothelial-Cell Specific Molecule-1 Binds Directly to the Integrin CD11a/CD18 (LFA-1) and Blocks Binding to Intercellular Adhesion Molecule-1[1]

David Béchard,* Arnaud Scherpereel,* Hamida Hammad,* Thibaut Gentina,* Anne Tsicopoulos,* Marc Aumercier,† Jöel Pestel,* Jean-Paul Dessaint,‡ André-Bernard Tonnel,* and Philippe Lassalle[2]*

ICAMs are ligands for LFA-1, a major integrin of mononuclear cells involved in the immune and inflammatory processes. We previously showed that endothelial cell specific molecule-1 (ESM-1) is a proteoglycan secreted by endothelial cells under the control of inflammatory cytokines. Here, we demonstrate that ESM-1 binds directly to LFA-1 onto the cell surface of human blood lymphocytes, monocytes, and Jurkat cells. The binding of ESM-1 was equally dependent on Ca^{2+}, Mg^{2+}, or Mn^{2+} divalent ions, which are specific, saturable, and sensitive to temperature. An anti-CD11a mAb or PMA induced a transient increase in binding, peaking 5 min after activation. Direct binding of ESM-1 to LFA-1 integrin was demonstrated by specific coimmunoprecipitation by CD11a and CD18 mAbs. A cell-free system using a Biacore biosensor confirmed that ESM-1 and LFA-1 dynamically interacted in real time with high affinity (K_d = 18.7 nM). ESM-1 consistently inhibited the specific binding of soluble ICAM-1 to Jurkat cells in a dose-dependent manner. These results suggest that ESM-1 and ICAM-1 interact with LFA-1 on binding sites very close to but distinct from the I domain of CD11a. Through this mechanism, ESM-1 could be implicated in the regulation of the LFA-1/ICAM-1 pathway and may therefore influence both the recruitment of circulating lymphocytes to inflammatory sites and LFA-1-dependent leukocyte adhesion and activation. *The Journal of Immunology,* **2001, 167: 3099–3106.**

Lymphocytes continuously patrol the body against foreign Ags by recirculating from blood through tissues into lymph and back to blood. They can circulate in a nonadherent form through blood and lymph but become adherent after receiving signals by inflammatory mediators, which activate adhesive mechanisms essential for immune responses (for reviews, see Refs. 1 and 2). Regulation of firm adhesion is controlled by many adhesion receptors; among them is the integrin family.

The LFA-1 is an $\alpha\beta$ heterodimeric transmembrane glycoprotein consisting of an α_L subunit (CD11a) and a β_2 subunit (CD18), not covalently bound, that physically link extracellular ligands to the cytoskeleton (3). The major counterreceptors for LFA-1 are ICAM-1, ICAM-2, and ICAM-3 (for review, see Ref. 4). The interaction between LFA-1 and ICAM-1 is of importance in a number of cellular events, including the regulation of leukocyte emigration from the blood into the tissues (5, 6) and in many intercellular cooperations during the specific immune response (7, 8). The beneficial effect obtained in vivo by blocking adhesion with mAbs in mouse and in other animal models clearly demonstrates that LFA-1 and ICAM-1 are involved in acute inflammation (9), ischemia/reperfusion injury (10), allograft rejection (11–13), and antitumor immunity. Consequently, an active search has been developed for molecules that antagonize LFA-1 and/or ICAM-1 functions. Among these molecules, soluble ICAM-1, peptides derived from ICAM-1, and blocking mAbs have been shown to reduce LFA-1-ICAM-1 interaction through the binding to the I domain of the α-chain, which leads to an inhibition of leukocyte adhesion in vitro (14–17). In contrast, a glycoprotein called neutrophil inhibitory factor has been shown to bind to CD11/CD18 integrins and to inhibit leukocyte adhesion (18), suggesting a novel pathway for endoparasites to escape from the host immune response. In addition, this molecule was able to reduce in vivo LPS-induced lung neutrophil infiltration.

In a previous work, we characterized a novel soluble chondroitin/dermatan sulfate proteoglycan called endothelial cell-specific molecule-1 (ESM-1),[3] which is secreted by endothelial cells.[4] Spontaneous expression of ESM-1 has been shown to be restricted to human lung and kidney tissues (19). Moreover, the expression of ESM-1 is differentially regulated by cytokines: TNF-α and IL-1β up-regulate and IFN-γ down-regulates the secretion of ESM-1, whereas IL-4 has no effect. Consistent with a basal secretion of ESM-1 by vascular endothelial cells, circulating ESM-1 is found in sera from healthy subjects and is increased in patients with acute and severe sepsis (20). The fact that ESM-1 is mainly released by the vascular endothelium, together with the differential

*Institut National de la Santé et de la Recherche Médicale Unité 416, Institut Pasteur de Lille; †Centre National de la Recherche Scientifique Unité Mixte de Recherche 8526, Institut de Biologie de Lille; and ‡Laboratoire d'Immunologie, Centre Hospitalier Régional Universitaire, Lille, France

Received for publication August 8, 2000. Accepted for publication June 29, 2001.

The costs of publication of this article were defrayed in part by the payment of page charges. This article must therefore be hereby marked *advertisement* in accordance with 18 U.S.C. Section 1734 solely to indicate this fact.

[1] This work was supported in part by Programme de Recherche en Santé PROGRES and Institut Fédératif de Recherche 17.

[2] Address correspondence and reprint requests to Dr. Philippe Lassalle, Institut National de la Santé et de la Recherche Médicale Unité 416, Institut Pasteur de Lille, 1 rue de Dr. A. Calmette, Boîte Postale 245, 59000 Lille, France. E-mail address: philippe.lassalle@pasteur-lille.fr

[3] Abbreviations used in this paper: ESM-1, endothelial cell-specific molecule-1; ESM/WT, wild-type ESM-1; MEC, mouse mAb to ESM-1 produced by Chinese hamster ovary cells; MFR, mean fluorescence ratio; MFI, mean fluorescence intensity; RU, resonance unit; GAG, glycosaminoglycan.

[4] D. Béchard, T. Gentina, M. Delehedde, A. Scherpereel, M. Lyon, M. Aumercier, R. Vazeux, C. Richet, P. Degand, B. Jude, A. Janin, D. G. Fernig, A. B. Tonnel, and P. Lassalle. Endocan is a novel chondroitin sulfate/dermatan sulfate proteoglycan which promotes hepatocyte growth factor/scatter factor mitogenic activity. *Submitted for publication*.

Copyright © 2001 by The American Association of Immunologists

0022-1767/01/$02.00

Downloaded from http://www.jimmunol.org/ by guest on March 21, 2019

regulation of its expression by proinflammatory cytokines, prompted us to examine the possibility that ESM-1 could affect the behavior of mononuclear cells. In the present work, we demonstrate that purified ESM-1 binds to human PBL and monocytes. Binding studies on several human leukocytic cell lines indicate that ESM-1 bound to a specific cell surface molecule on Jurkat cells. Coimmunoprecipitation and Biacore analysis identified the β_2 integrin LFA-1 as the specific receptor of ESM-1, and ESM-1 was shown to inhibit the binding of soluble ICAM-1 to Jurkat cells. Therefore, ESM-1 is an extracellular ligand for LFA-1 and may be considered as a soluble immunomodulator of the LFA-1/ICAM-1 pathway.

Materials and Methods

Reagents, cell lines, and cell culture

Anti-CD11a (clone HI111 (blocking) and clone G43-25B (nonblocking)), anti-CD11b (clone ICRF44), anti-CD18 (clone 6.7), anti-CD2, and anti-CD3 mAbs were purchased from BD PharMingen (San Diego, CA). Anti-CD44 mAb was purchased from Sigma-Aldrich (St. Louis, MO). CM5 Sensor Chips were obtained from Biacore (Uppsala, Sweden). The development of HEK293 cell lines expressing the wild type of ESM-1 (ESM/WT) has been previously described.[4] ESM/WT was produced by an established cell line called 293-ESM. ESM/WT from conditioned cell supernatants without FCS was purified sequentially by ion exchange chromatography (DEAE-Sepharose) followed by immunoaffinity chromatography with a mouse mAb to ESM-1 produced by Chinese hamster ovary cells (MEC)-4 mAb Hz-agarose column (Bio-Rad, Hercules, CA) (see *Production of anti-ESM-1 mAbs* below). The bound material was then eluted in 3 M $MgCl_2$, concentrated, dialysed, and stored at −70°C. The protein level was evaluated by Bio-Rad assay, Coomassie blue-, or Alcian blue- stained SDS-PAGE. The ESM-1 level was assessed by ELISA. The level of endotoxin was checked by *Limulus* amebocyte lysate assay. Aliquots of 200 ng/ml ESM-1 in PBS containing 0.1% BSA were kept frozen at −70°C and served for the standard curve ranging from 0.1 to 10 ng/ml. The lymphoblastic cell lines Jurkat and SIB-1, monocytic cell line U937, and myelocytic cell line HL60 were cultured in RPMI 1640 medium with 10% FCS and 2 mM L-glutamine. The monocytic cell line THP1 was cultured in DMEM, 10% FCS, and 2 mM L-glutamine. Transfected and established cell lines producing soluble ESM-1 and soluble ICAM-1 (293-ESM and 293–3D-ICAM-1/Fc) were cultured in DMEM 10% FCS, and 2 mM L-glutamine. PBMC were obtained from healthy individual volunteers after Ficoll gradient centrifugation (Pharmacia Biotech, Uppsala, Sweden). Mononuclear cells were resuspended in RPMI 1640 supplemented with 10% FCS, 2 mM L-glutamine, and antibiotics.

Production of anti-ESM-1 mAbs

To obtain anti-ESM-1 mAbs against the cysteine-rich region of ESM-1, the native form of ESM-1 was purified from an established Chinese hamster ovary-ESM cell line. BALB/c mice were immunized (10 μg/mouse) with a standard immunization protocol using CFA. Hybridoma cells secreting anti-ESM-1 mAbs were obtained by fusion, screening, and subcloning as previously described (20). Five hybridoma cell clones were obtained and were called MEC. Four of them were of IgG1, k isotype (MEC 4, 5, 15, and 36), and one of them was of IgM, k isotype (MEC 11). The hybridoma clones were cultured in serum-free medium, and anti-ESM-1 mAbs were purified on protein G-Sepharose chromatography (Pharmacia Biotech).

Flow cytometric analysis

Binding of ESM-1 to PBMC and Jurkat cells was analyzed on a FACScalibur (BD Biosciences, San Jose, CA). A total of 500,000 cells were incubated with or without 300 ng/ml purified ESM-1 in incubating buffer containing PBS, 1 mM $CaCl_2$, 1 mM $MgCl_2$, 1 mM $MnCl_2$, and in some experiments, 5 mM EDTA for 1 h at 4°C. Cells were washed three times in buffer and incubated with an anti-ESM-1 mAb, MEC 15, vs an isotype-matched mouse IgG1 as a negative control for 30 min at 4°C. After washing, cells were incubated with a FITC-anti-mouse IgG at 1/100 and washed three times before FACS analysis. Mean fluorescence ratio (MFR) was calculated by dividing mean fluorescence intensity (MFI) of the sample by the MFI of the control; thus, a MFR of 1 is equivalent to background.

Quantitative binding evaluation

To evaluate the binding of ESM-1 to different leukocytic cell lines, $\sim 1 \times 10^7$ cells (Jurkat, SIB-1, THP1, U937, and HL60) were incubated in 2 ml RPMI 1640 medium containing 300 ng/ml purified ESM-1 for 1 h at 4°C. Cells were centrifuged at 1500 rpm for 5 min at 4°C, washed three times in ice-cold buffer without ESM-1, and lysed at 4°C in 500 μl of lysis buffer containing PBS, complete anti-proteases mixture with EDTA (Boehringer Mannheim, Mannheim, Germany), and 0.5% Nonidet P-40 (Boehringer Mannheim). After removal of insoluble material by centrifugation at 10,000 rpm for 15 min, bound ESM-1 was quantified by a specific ELISA (20). In some experiments, the binding of ESM-1 to Jurkat cells was performed at 37°C. The cell suspension, preheated to 37°C, was activated with PMA (100 ng/ml) for various periods of time from 5 to 30 min. The tubes were then cooled on ice, incubated with ESM-1 for 1 h at 4°C, and then washed with ice-cold incubating medium. To evaluate the divalent ion dependence of the binding, Jurkat cells were incubated in PBS containing either 1 mM $CaCl_2$, 1 mM $MgCl_2$, or 1 mM $MnCl_2$ in the presence of 300 ng/ml purified ESM-1 for 1 h at 4°C. Jurkat cells were also incubated in RPMI 1640 medium containing 300 ng/ml purified ESM-1, with or without 5 mM EDTA, for 1 h at 4°C.

Coimmunoprecipitation procedure

Approximately 5×10^7 Jurkat cells were incubated in 10 ml of RPMI 1640 complemented with purified ESM-1 at a concentration of 300 ng/ml with $MgCl_2$, $MnCl_2$, and $CaCl_2$ at 1 mM each for 1 h at 4°C. Then cells were washed three times in ice-cold RPMI 1640 medium and were lysed in 500 μl of a specific lysis buffer (PBS and EDTA-free complete anti-proteases mixture, 1 mM $MgCl_2$, 1 mM $MnCl_2$, 1 mM $CaCl_2$, and 5 mM octylthioglucoside (Boehringer Mannheim) for 30 min at 4°C. After removal of insoluble material by centrifugation at 10,000 rpm at 4°C, supernatants were incubated with 6 μg of different mouse mAbs at 4°C. After 2 h, 150 μl of anti-mouse Fc agarose beads were added during 1 h at 4°C. Then beads were washed three times in lysis buffer by centrifugation at 2500 rpm at 4°C. Next, beads were eluted with 200 μl of 3 M $MgCl_2$ for 10 min at room temperature. After rapid centrifugation, 200 μl of eluate was resuspended with 3 ml of PBS containing 1 tablet of complete anti-proteases mixture. Eluate was desalted and was concentrated on 30-kDa centricon (Amicon, Beverly, MA). ESM-1 was quantified by using a specific ELISA. The cell membrane-associated molecules from Jurkat cells were considered conserved in their functional status based on the optimization of the solubilization procedure. In particular, the solubilized LFA-1 molecule was verified to be heterodimeric by Biacore and differential immunoprecipitation immunoblot procedures (data not shown).

Real-time bimolecular interaction assay

The Biacore system was used. In this system, binding of soluble ligands to immobilized ligands was measured in arbitrary units (resonance units, RU). There was a linear relationship between the mass of the protein bound to the immobilized protein and the RU observed (1000 RU = 1 ng/mm^2 bound protein). An anti-CD11a (HI111) mouse mAb was immobilized at 8000 RU to the carboxymethylated dextran matrix of the sensor chip according to the manufacturer's protocol using the Amine Coupling Kit (Biacore) and was compared with a control surface (activated and blocked sensor surface). LFA-1 molecules from the Jurkat lysates could only be fixed by immunoaffinity procedure. Approximately 2×10^8 Jurkat cells were lysed in 2 ml of lysis buffer (PBS, 1 mM $MgCl_2$, 1 mM $MnCl_2$, complete anti-proteases mixture (EDTA-free), and 5 mM octylthioglucoside) for 30 min at 4°C. After removal of insoluble material by centrifugation and incubation in a sonication bath, the lysate was injected at a flow rate of 5 μl/min for 30 min at 25°C to immobilize approximately 1500 RU LFA-1 molecules. Next, CD11a mAb (G43-25B), CD18 mAb, and purified ESM-1 were diluted in running buffer (PBS, 1 mM $MgCl_2$, and 1 mM $MnCl_2$) and injected at a flow rate of 5 μl/min for 5 min at 25°C. The K_a and K_d were calculated according to the BIAevaluation software version 3.1 provided by the manufacturer. The affinity constant was calculated from the equation $K_d = K_d/K_a$.

Metabolic radioisotope labeling of soluble ICAM-1/Fc

A form of ICAM-1/Fc chimeric protein consisting of the three first extracellular domains of ICAM-1 fused to the Fc fragment of human IgG1 was expressed in 293 cells as previously described (20). Exponentially growing adherent cultures (293–3D-ICAM-1/Fc cells) were washed twice in a methionine and cysteine-free DMEM containing 5% dialysed FCS and were incubated in this medium for 2 h at 37°C. The medium was then changed to methionine and cysteine-free DMEM supplemented with [^{35}S]methionine (50 μCi/ml of medium and 1175 Ci/mmol ^{35}S-labeled TransLabel, ICN Pharmaceuticals) overnight at 37°C. Supernatants were cleared by centrifugation at 2000 rpm for 5 min and were loaded on an anti-human Fc-agarose column according to the manufacturer's recommendations

Downloaded from http://www.jimmunol.org/ by guest on March 21, 2019

(Bio-Rad). Soluble ICAM-1 was eluted in 3 M $MgCl_2$, desalted, and concentrated on 30-kDa centricon. Concentration of soluble ICAM-1 was determined by using a specific soluble ICAM-1 ELISA (Diaclone, Besançon, France). A ratio of amount:cpm was obtained, and the specific activity was ~75,000 cpm/μg.

Analysis of the binding of soluble ICAM-1/Fc to Jurkat cells

Jurkat cells were incubated in RPMI 1640 medium supplemented or not with ESM-1 at a concentration of 300 ng/ml for 1 h at 4°C. Cells were washed twice in RPMI 1640 medium and incubated in medium supplemented with radiolabeled soluble 3D-ICAM-1/Fc (1 μg/ml) for 30 min either at 4°C or at 37°C. Cells were washed twice with medium heated at corresponding temperatures and resuspended in 2 ml of scintillation liquid. Binding of soluble 3D-ICAM-1/Fc was evaluated by cpm counting in a Beckman counter (Beckman, Rouissy, CDG, France). To determine the optimal effect of ESM-1, some experiments were conducted with increasing concentrations of ESM-1 ranging from 1 to 1000 ng/ml incubated with Jurkat cells before 3D-ICAM-1/Fc binding.

Results

ESM-1 binds to the surface of PBMC and Jurkat cells

To study the possibility that ESM-1 may interact with PBMC obtained from healthy volunteers, we explored the binding ability of ESM-1 to PBMC by flow cytometric analysis. When human PBMC were incubated with ESM-1, a consistent and specific binding to the cell surface of human lymphocytes (MFI = 12.07 ± 2.3; MFR = 2.9) was observed as compared with the cells not incubated with ESM-1 (MFI = 4.12 ± 0.9). In addition, human monocytes also bound ESM/WT (MFI = 25.59 ± 3.6; MFR = 1.7) as compared with control monocytes (MFI = 14.78 ± 1.3) (Fig. 1). To better characterize the cell surface binding of ESM-1, several cell lines (Jurkat and SIB-1 lymphoblastoid, U937 and THP1 monocytoid, and HL60 myeloid cell lines) were examined for their ability to bind ESM-1. As shown in Fig. 1, ESM-1 bound to the cell surface of Jurkat cells (MFI = 7.51 ± 0.8; MFR = 3.4) as compared with Jurkat cells not incubated with ESM-1 (MFI = 2.22 ± 0.5). SIB-1 cells, a B lymphoblastoid cell line, also bound ESM-1 to a similar extent as Jurkat cells. In contrast, U937, THP1, and HL60 cells did not show any significant ESM-1 binding (data not shown). To quantify the presence of ESM-1 on the cell surface, bound ESM-1 was released by complete cell lysis and was evaluated by a specific ELISA. In a resting state, only Jurkat and SIB-1 lymphoblastoid cell lines were able to bind constitutively and significantly to ESM-1 (Fig. 2). The results are in agreement with the MFR, suggesting that ESM-1 in cell lysates reflected the cell surface-bound ESM-1. It is unlikely that the ESM-1 level in cell lysates was related to an endocytic form of ESM-1 because all the experiments were performed on ice, and monocytoid cell lines were negative. In contrast, no ESM-1 or related forms were detected by RT-PCR and specific ELISA, discarding any endogenous synthesis and expression of ESM-1, but suggesting the presence of a specific receptor for ESM-1 on their surface.

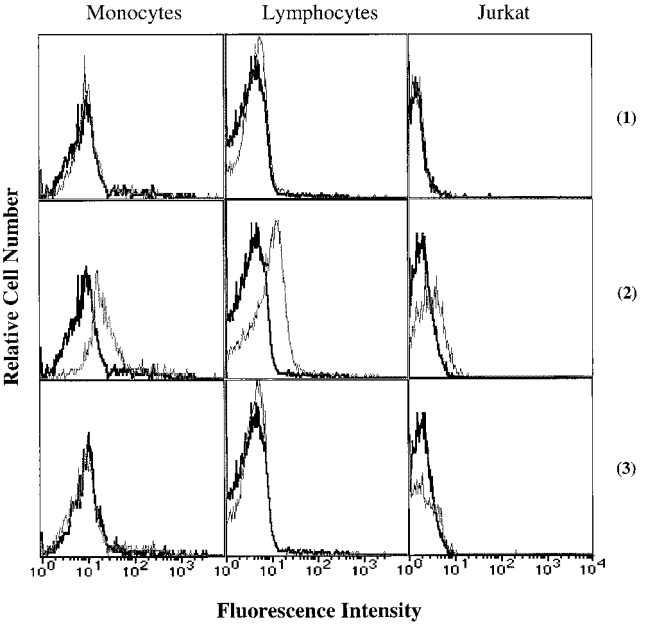

FIGURE 1. ESM-1 binds specifically to the cell surface of human lymphocytes, monocytes, and Jurkat cells. Lymphocytes, monocytes, and Jurkat cells bound consistently and specifically ESM/WT, and this binding activity disappeared in the presence of EDTA. PBMC and Jurkat cells were incubated either in the presence of purified ESM/WT (*2*), EDTA (5 mM) plus ESM/WT (*3*), or buffer alone (*1*) for 1 h at 4°C. Bound ESM-1 was detected by a specific MEC15 mAb (clear line) vs an isotype-matched IgG1 as negative control (bold line) followed by a FITC-conjugated anti-mouse IgG and was then analyzed by flow cytometry. This experiment is representative of three independent experiments.

Binding of ESM-1 on Jurkat cells is divalent ion-dependent and saturable

The binding of ESM-1 to Jurkat cells was completely abolished by the presence of EDTA in the medium (Figs. 1 and 3*A*). Incubation of Jurkat cells with purified ESM-1 in PBS alone did not lead ESM-1 to bind. In contrast, the single addition of either Ca^{2+}, Mg^{2+}, or Mn^{2+} ions in PBS medium was able to restore the binding of ESM-1 to Jurkat cells in a similar fashion for each of the three divalent ions (Fig. 3*B*). Dose-response curves of bound ESM-1 were titrated in the presence or absence of EDTA. The amount of bound ESM-1 that was divalent ion dependent was obtained after subtraction of the amount of ESM-1 bound. The resulting curve demonstrated that bound ESM-1 reached a plateau beginning at 4 nM (Fig. 3*C*). Experiments conducted with 2×10^7 and 5×10^7 cells/point gave curves with a similar plateau. These results point to the presence of a divalent ion-dependent and saturable binding site for ESM-1 on the surface of Jurkat cells.

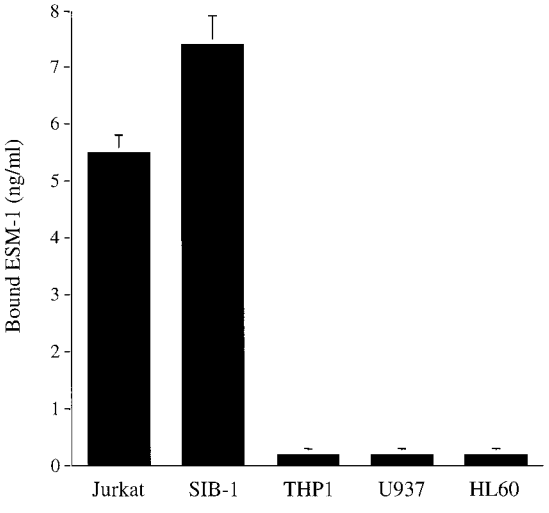

FIGURE 2. Analysis of the binding of ESM-1 to different leukocytic cell lines. ESM-1 specifically binds to the lymphoblastoid cell lines. Binding studies of ESM-1 were performed on lymphoblastoid cell lines (Jurkat and SIB-1), monocytoid cell lines (THP1 and U937), and a myeloid cell line (HL60), each in resting state. Cells were incubated in the presence of ESM/WT for 1 h at 4°C, and detection of their bound ESM-1 was quantified in cell lysates by a specific ELISA. Data (n = 5) are expressed in nanograms per milliliter ESM-1 from a 500-μl total volume of cell lysate.

Downloaded from http://www.jimmunol.org/ by guest on March 21, 2019

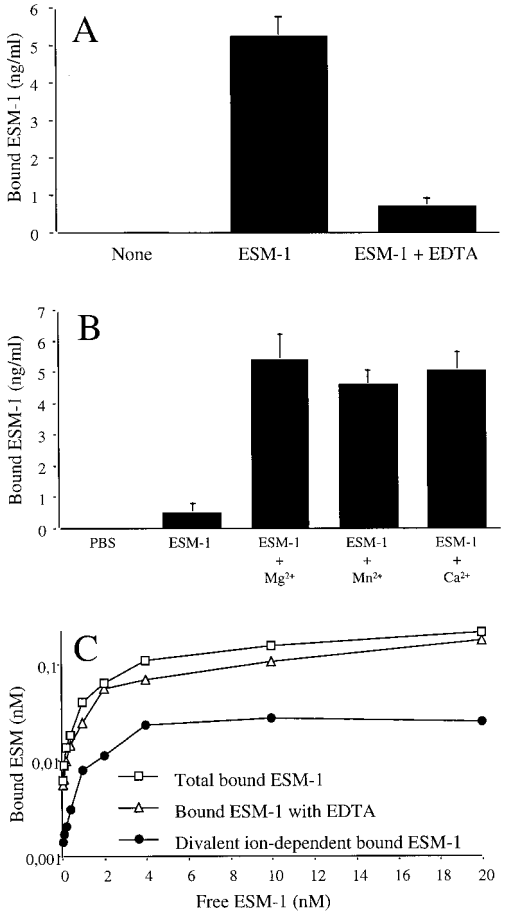

FIGURE 3. Characterization of the divalent ion-dependent and saturable binding of ESM-1 to the membrane. *A*, Abolition of the binding of ESM-1 in the presence of EDTA. Jurkat cells were incubated with ESM-1 with or without 5 mM EDTA. Cells were washed and lysed. Bound ESM-1 was evaluated by a specific ELISA in lysates ($n = 5$). *B*, Divalent ions restore the binding activity of ESM-1 to Jurkat cells. Binding studies were done in PBS alone or supplemented with different divalent ions (Mg^{2+}, Mn^{2+}, and Ca^{2+}). Cells were washed and lysed. Bound ESM-1 was evaluated by a specific ELISA in lysates ($n = 5$). *C*, The cell surface binding of ESM-1 to Jurkat cells is saturable. Approximately 1×10^7 Jurkat cells were incubated with increasing concentrations of ESM-1 in the presence or the absence of EDTA for 1 h at 4°C, then washed and lysed. Bound ESM-1 was detected by specific ELISA in lysates. Bound ESM-1 in the presence of EDTA was subtracted from bound ESM-1 in the absence of EDTA. The resulting curve represents the divalent ion-dependent bound ESM-1. This curve reached a plateau for an ESM-1 free concentration of 4 nM. This experiment is representative of three distinct experiments.

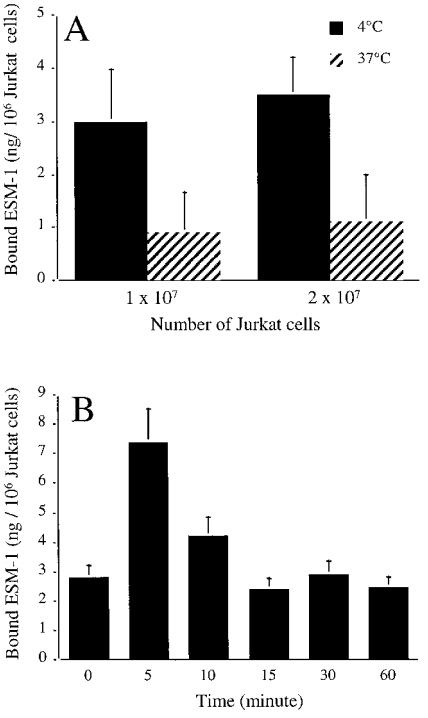

FIGURE 4. Effects of temperature and PMA activation on ESM-1 binding to Jurkat cells. *A*, Decreased binding of ESM-1 at 37°C. A total of $10–20 \times 10^6$ Jurkat cells were incubated with ESM-1 either at 4°C or 37°C for 1 h and then washed three times with RPMI 1640 buffer at the respective temperatures. Results are expressed as mean ± SD of three experiments. *B*, Transient increase in bound ESM-1 upon PMA activation. Approximately 1×10^7 Jurkat cells were incubated at 37°C for various periods of time with PMA (100 ng/ml) or with medium alone. The cells were quickly cooled on ice and subjected to the ESM-1-binding assay at 4°C. Results are expressed as mean ± SD of three experiments.

Role of temperature and PMA activation

The effect of temperature on ESM-1 binding to Jurkat cells was also evaluated. The binding of ESM-1 at 37°C still persisted but to a lesser extent than at 4°C (Fig. 4*A*). Identical results were obtained with two different cell concentrations. Nearly half the quantity of bound ESM-1 was lost by shifting the binding temperature from 4°C to 37°C. Binding experiments with D-[6-^{3}H]glucosamine-labeled ESM-1 gave a similar result: a reduced level of bound radioactivity at 37°C (51 cpm) compared with that detected at 4°C (370 cpm, data not shown). These results suggest that membrane fluidity, metabolic energy, or internalization are involved in the dissociation of bound ESM-1 from Jurkat cells. To appreciate a possible modulation of ESM-1-binding activity, Jurkat cells were activated nonspecifically by PMA. Kinetics of activation showed a rapid increase at 5 min of incubation with PMA (Fig. 4*B*), with a normalization of the ESM-1 binding after 15 min of activation, arguing for the presence at the surface of Jurkat cells of a regulated binding site for ESM-1.

Anti-LFA-1 mAb coimmunoprecipitates ESM-1 and LFA-1 and enhances the binding of ESM-1 to Jurkat cells

To identify the binding site of ESM-1, we focused on the β_2 integrins because of some amino acid sequence homologies between ESM-1 and the cysteine-rich region of CD18 (19). This led us to speculate that ESM-1 might bind to the α-chain of β_2 integrins, the most interesting candidates because they are expressed on both PBMC and Jurkat cells. ESM-1 was reproducibly coimmunoprecipitated from Jurkat cells by the anti-ESM-1 mAb clone MEC15 (positive control) (14.1 ± 3.2 ng/ml) and, interestingly, also by the anti-CD11a mAb clone HI111 (4.8 ± 0.8 ng/ml) and by an anti-CD18 mAb (4.6 ± 1.1 ng/ml) (Fig. 5*A*). However, anti-CD11a mAbs were differentially able to coimmunoprecipitate bound ESM-1; the blocking anti-CD11a mAb (clone HI111), which is known to inhibit the binding of ICAM-1, coimmunoprecipitated ESM-1, whereas the nonblocking anti-CD11a mAb (clone G43-25B) was inefficient, despite similar MFIs obtained by FACS. To test whether anti-CD11a mAbs could modify the binding of ESM-1 to Jurkat cells, Jurkat cells were incubated first with different mAbs and then subjected to ESM-1-binding analysis. Surprisingly, as shown in Fig. 5*B*, the anti-CD11a mAb (clone HI111), in the presence of divalent ions, led to a consistent increase in ESM-1 binding (17.2 ± 1.5 ng/ml), as compared with controls in absence of specific mAb (5.8 ± 0.3 ng/ml) and with the

Downloaded from http://www.jimmunol.org/ by guest on March 21, 2019

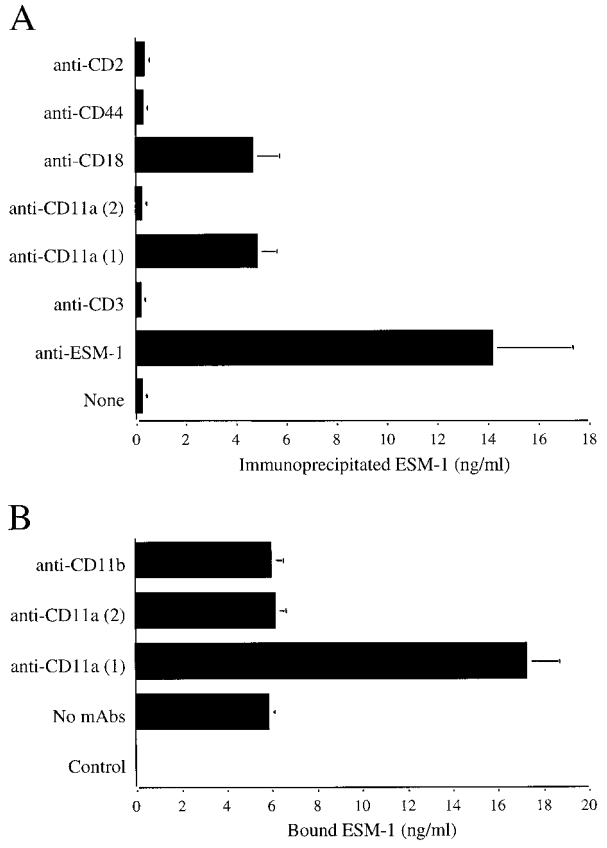

FIGURE 5. An anti-CD11a mAb coimmunoprecipitates ESM-1 with LFA-1 and increases ESM-1 binding to Jurkat cells. *A*, Coimmunoprecipitation of ESM-1 with LFA-1. Jurkat cells were incubated with ESM-1 for 1 h at 4°C, and immunoprecipitations were done with different mAbs according to the procedure previously described (none; anti-ESM-1 (MEC15); anti-CD3; anti-CD11a (1), i.e., clone HI111; anti-CD11a (2), i.e., clone G43-25B); anti-CD18; anti-CD44; and anti-CD2). Beads were washed and eluted. ESM-1 contents from eluates were analyzed by a specific ELISA. ESM-1 was not coimmunoprecipitated by anti-CD44, anti-CD3, and anti-CD2 mAbs despite their expression at the surface of Jurkat cells, as checked by FACS analysis. *B*, Activation of the binding of ESM-1 by an anti-CD11a mAb. Jurkat cells were first incubated in binding medium with different mAbs (anti-CD11a HI111 (1), anti-CD11a G43-25B (2), and anti-CD11b for 1 h at room temperature and secondly with ESM-1 or without ESM-1 (control) for 1 h at 4°C. Cells were washed and lysed. ESM-1 was quantified by a specific ELISA in lysates ($n = 5$).

isotype-matched nonblocking G43-25B control, anti-CD11a mAb (6.1 ± 0.5 ng/ml). These results demonstrate a physical association between ESM-1 and LFA-1 and that the binding of ESM-1 may be regulated by the specific anti-CD11a mAb clone HI111.

Real-time interaction between LFA-1 and ESM-1

To better define the interaction between LFA-1 and ESM-1, a real-time observation by Biacore analysis was conducted. The Sensor Chip was filled with detergent lysates of Jurkat cells to capture functional LFA-1 molecules. Specific binding of the heterodimeric form of LFA-1 to the anti-CD11a mAb-coupled Sensor Chip was observed, which is essential to keep LFA-1 functional (Fig. 6*A*). Then, we examined the interaction of LFA-1 and purified human ESM-1. An overlay of sensor-grams for the binding of ESM-1 to LFA-1 is shown in Fig. 6*B*. Sensor-grams showed two phases: a fast association phase, detected when purified human ESM-1 was injected and was allowed to bind to the immobilized LFA-1 (0–250 s), and a slow dissociation phase, in which the ESM-1 solution

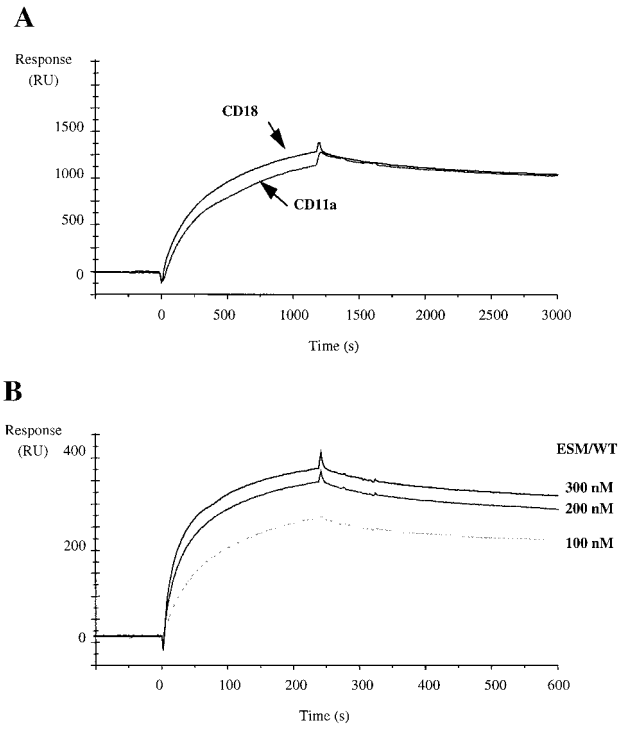

FIGURE 6. Real-time observation of ESM-1-LFA-1 interaction. *A*, Overlay sensor-grams from the Biacore analysis demonstrating the capture on the chip of LFA-1 under its heterodimeric form. The heterodimeric CD11a/CD18 molecules were filled on the Sensor Chip by interacting with a covalently bound anti-CD11a mAb (HI111) in a first step. The capture of both CD11a and CD18 chains was checked by injection of another anti-CD11a mAb (G43-25B) or an anti-CD18 mAb as the analyte. Arrows indicate the detection of the CD11a and the CD18 chains. Data are representative of three separate experiments. *B*, Overlay sensor-grams showing the binding of purified human ESM-1 to LFA-1 by Biacore analysis. Purified ESM-1 was injected in the LFA-1 precaptured channel at the following concentrations: 100, 200, and 300 nM during 250 s. Next, the analyte was replaced by running buffer as described in *Materials and Methods*. K_a and K_d were fitted by using the BIAevaluation software (version 3.1) to determine K_D.

was replaced with running buffer (250–600 s). The association and dissociation phases were fitted and linearized according to the BIAevaluation software (version 3.1). The K_a calculated from five distinct concentrations (from 50 to 300 nM) was 4.41×10^4 $M^{-1}s^{-1}$, and the K_d) was $8.25 \times 10^{-4}s^{-1}$. K_D, calculated from the ratio of the rate constants, was 18.7×10^{-9} M.

ESM-1 inhibits the binding of soluble ICAM-1 to Jurkat cells

The fact that ESM-1 interacted with LFA-1 suggests that ESM-1 might interfere on LFA-1-ICAM-1 interactions. To explore this hypothesis, metabolically labeled and affinity-purified 3D-ICAM-1/Fc (soluble ICAM-1) was used. The specific binding of ICAM-1 to Jurkat cells (4652 ± 156 cpm) was strongly inhibited by the blocking anti-CD11a mAb clone HI111 (837 ± 168 cpm), indicating that in our experimental model, almost all the labeled ICAM-1 was bound to LFA-1 (Fig. 7*A*). When ESM-1 was coincubated with soluble ICAM-1 and the Jurkat cells, we observed an inhibition of specific binding of soluble ICAM-1 of 64 ± 9% (2200 ± 139 cpm). This inhibitory effect appeared dose-dependent, reaching a plateau at 300 ng/ml (Fig. 7*B*). At 37°C, the binding capacity of 3D-ICAM-1/Fc on Jurkat cells was reduced (1419 ± 165 cpm); however, ESM-1 still inhibited ICAM-1 binding (772 ± 88 cpm; 46 ± 9%; Fig. 7*A*). Based on a molecular mass

Downloaded from http://www.jimmunol.org/ by guest on March 21, 2019

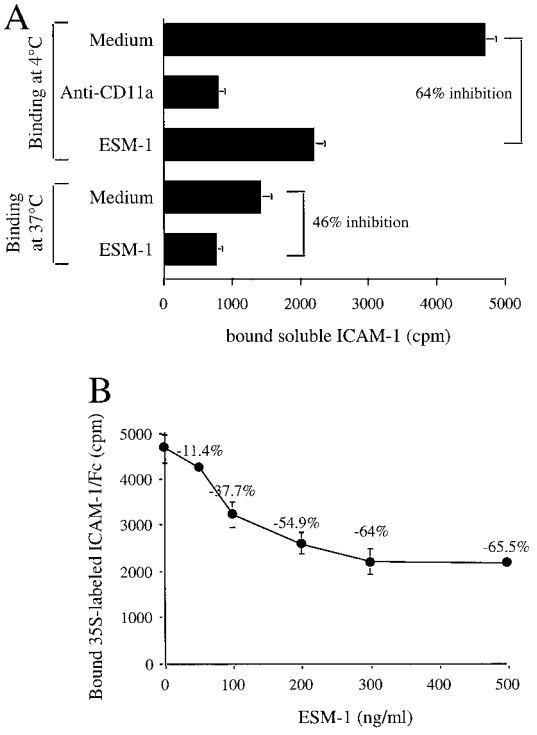

FIGURE 7. ESM-1 inhibits soluble ICAM-1 binding to Jurkat cells. *A*, Effect of temperature. Jurkat cells were incubated with or without ESM-1 at 300 ng/ml or with blocking CD11a mAb at 1 μg/ml in the presence of radiolabeled soluble ICAM-1 for 1 h either at 4°C or at 37°C. Cells were washed, and the binding of soluble ICAM-1 was measured by liquid scintillation counting. Anti-CD11a (clone HI111) strongly blocked the specific binding of soluble ICAM-1 to LFA-1 on Jurkat cells. ESM-1 was able to reduce the specific binding of soluble ICAM-1 by 64 $\pm$ 11% at 4°C (n = 5) and by 46 $\pm$ 9% at 37°C (n = 3). *B*, Dose-response inhibition of ICAM-1 binding by ESM-1. Results are expressed in cpm of ^{35}S-labeled 3D-ICAM-1/Fc bound to Jurkat cells (mean $\pm$ SD from two to three experimental data for each point). Experiments were performed at 4°C. The mean percentage of inhibition is indicated for each point.

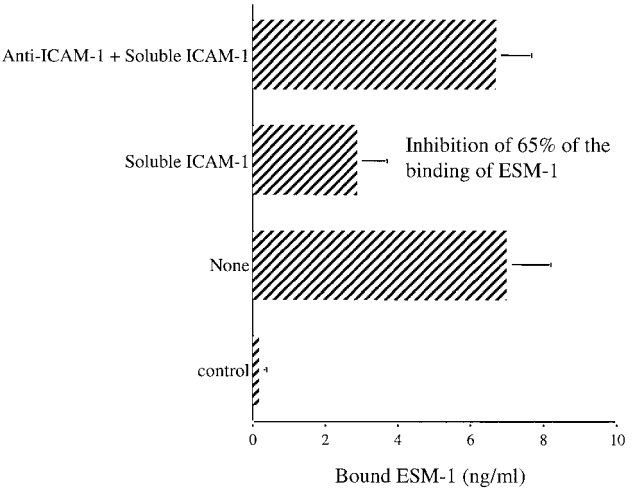

FIGURE 8. Soluble ICAM-1 inhibits ESM-1 binding to Jurkat cells. Jurkat cells were incubated with or without soluble ICAM-1 at 300 ng/ml or soluble ICAM-1 supplemented with blocking ICAM-1 mAbs at 1 μg/ml in the presence of ESM-1 at 300 ng/ml or not (control). ESM-1 binding was evaluated by a specific ELISA. Soluble ICAM-1 inhibited the binding of ESM-1 to Jurkat cells of 65 $\pm$ 13%, and this inhibitory effect was specifically abolished by coincubation with blocking anti-ICAM-1 mAbs (n = 5).

of 50 kDa, as observed on Western blot, 300 ng/ml ESM-1 is equal to 1.7×10^{-8} M and fits the K_d value determined by Biacore analysis (1.87×10^{-8} M). Conversely, the ability of soluble ICAM-1 to inhibit the binding of ESM-1 to Jurkat cells was explored. The preincubation of Jurkat cells with 3D-ICAM-1/Fc decreased the binding of ESM-1 by 65% (2.9 $\pm$ 0.3 ng/ml) as compared with controls (7.2 $\pm$ 0.4 ng/ml). However, the pretreatment of 3D-ICAM-1/Fc with a blocking anti-ICAM-1 mAb totally restored the binding of ESM-1 to Jurkat cells (6.7 $\pm$ 0.6 ng/ml) (Fig. 8). It is unlikely that ESM-1 had the capacity to bind to the soluble 3D-ICAM-1/Fc because ESM-1 was not coprecipitated by 3D-ICAM-1/Fc. Thus, these data demonstrate that ESM-1 and ICAM-1 can compete for the binding to LFA-1, and consequently, ESM-1 might modulate the interaction of LFA-1 and ICAM-1.

Discussion

The present work demonstrates that ESM-1, which is mainly secreted by endothelial cells, interacts physically and functionally with the extracellular domain of the LFA-1 integrin on Jurkat cells and plays a role in the regulation of LFA-1-mediated interactions.

ESM-1 is a chondroitin/dermatan sulfate proteoglycan produced by HUVECs. Its secretion is regulated by cytokines, and it circulates into the bloodstream (20). Because of its constitutive and cytokine-regulated expression restricted to endothelial cells, a role for ESM-1 in endothelial cell-leukocyte interactions has been postulated. In an initial search for a cell surface receptor for ESM-1, we observed that human blood mononuclear cells and two human lymphoblastoid cell lines exhibited specific ESM-1-binding activity as demonstrated by FACS analysis. Interestingly, ESM-1 bound to purified blood lymphocytes and to resting T and B resting lymphoblastoid cell lines, Jurkat and SIB-1 cells, respectively.

To biochemically characterize the binding sites for ESM-1, the model of the Jurkat cell line was used. We found that the binding of ESM-1 to Jurkat cells was mostly dependent on the presence of divalent ions. This divalent ion-dependent binding of ESM-1 was saturable, consistent with a receptor-like structure. Coimmunoprecipitations demonstrated that ESM-1 was solely coimmunoprecipitated by anti-LFA-1 mAbs. The interaction between ESM-1 and LFA-1 was specific because ESM-1 was not recovered with mAbs directed against other T cell surface molecules such as CD3 and CD44, despite their concomitant expression in the same membrane raft clusters (21). The very low expression of CD11a at the surface of the monocytoid cell lines used may explain the absence of binding of ESM-1. Direct interaction between ESM-1 and LFA-1 was then studied using the Biacore biosensor system. Measurement of the rate constants demonstrated a physical interaction between ESM-1 and LFA-1 with a K_d of 18.7 nM, close to that observed for soluble ICAM-1 and LFA-1 of 60 nM (22), highly consistent with a direct interaction between ESM-1 and LFA-1.

The mapping of the ESM-1 binding site within the LFA-1 molecule was also investigated. Among the two CD11a and the CD18 mAbs tested, two of them are known to block LFA-1-ICAM-1 interaction, but none of them was able to inhibit ESM-1 binding. It can be suggested that the ESM-1 binding site is not identical with the sites involved in LFA-1-ICAM-1 interactions (i.e., the I domain) (23). However, the ESM-1-binding capacity of Jurkat cells was shown to be increased by one LFA-1 mAb (HI111 clone) in the presence of divalent ions; this result reveals that the binding site for ESM-1 can be functionally regulated. The fact that significant amino acid sequence homology does exist between ESM-1 and the cysteine-rich repeats of CD18 suggests that ESM-1 may possibly interact with LFA-1 through its polypeptide moiety in or near this functionally important region (24, 25).

Downloaded from http://www.jimmunol.org/ by guest on March 21, 2019

One interesting point is that some differences appeared between the binding characteristics of the couples ESM-1 and LFA-1 and ICAM-1 and LFA-1. In contrast to ICAM-1, the binding of ESM-1 to Jurkat cells was higher at 4°C than at 37°C. Detailed analysis of this difference has not been addressed. Another difference with ICAM-1 was an increase in ESM-1 binding induced by PMA. Maximal binding occurred at 5 min and quickly returned to baseline after 15 min of activation. This pattern more closely resembles the kinetics of TCR-stimulated T cell adhesion to ICAM-1, which peaks at 10 min with a complete return to the low adhesiveness state by 30 min., than PMA stimulation of LFA-1-ICAM-1 adhesion, which is maximal at 10 min and remains high for up to 30 min. (26). These results suggest that the ESM-1 binding site is sensitive to the activation status of LFA-1. They also suggest that among the different conformational states during LFA-1 activation, one of the earliest activation steps should include an upregulation of the ESM-1 binding site.

We have also investigated the consequences of the binding of ESM-1 on LFA-1-ICAM-1 interaction. We have found that ESM-1 significantly reduced the binding of soluble 3D-ICAM-1/Fc to Jurkat cells. Inversely, the soluble 3D-ICAM-1/Fc was shown to reduce the binding of ESM-1 to Jurkat cells. These results indicate that ESM-1 and ICAM-1, although presumably binding to nonidentical sites, can alter LFA-1 conformation to block each other's binding. ESM-1 is a soluble proteoglycan containing one single chain of glycosaminoglycan (GAG).[4] It has been already shown that GAG chains from proteoglycans can bind $\alpha_4\beta_1$ integrin through a specific binding site that can be activated by Mn^{2+} ions (27). Yet, such a direct binding of GAG to LFA-1 integrin has not been documented. Moreover, the lysine-rich specific binding site for GAG found in the α_4 sequence is not present in the LFA-1 primary sequence. However, the GAG chain of ESM-1 is sulfated, and these sulfate ions might be involved through their association to the LFA-1-fixed divalent ions and interfere with ICAM-1 binding.

The LFA-1 molecule contains specific divalent ion binding sites called metal ion-dependent adhesion site motifs in the conserved region of the extracellular domain of the CD18 chain, in the I domain of the CD11a chain (23), and in the EF hand-like domains. They are essential to regulate the fully activated phenotype of the integrin. Many studies indicate that Ca^{2+} down-regulates the activated state of LFA-1 for ICAM-1 (28–31), whereas Mg^{2+} and Mn^{2+} favor conformational changes and appearance of ligand-induced binding sites to obtain the optimal fully activated state of LFA-1 (32–33). In our experimental conditions, such a down-regulation by Ca^{2+} of ESM-1 binding was not observed; all the three ions equally increased the binding of ESM-1 to Jurkat cells. A similar ion-dependent effect was observed for ESM-1 binding to PBMC, indicating that the ESM-1 binding sites to PBMC and to Jurkat cells shared common features. On a theoretical point of view, ICAM-1 binding to LFA-1 is divided into ligand-binding and ion-binding steps. In the first step, ICAM-1 binds with low affinity to the conserved region of CD18 and the I domain of LFA-1, inducing sequential and conformational changes and access of Mg^{2+} and Mn^{2+} ions to their binding sites. Then, the second step occurs through ICAM-1 binding to the two last binding sites localized in the β sheets of the β propeller (34), leading to the high affinity interaction. Here, we can propose that ESM-1 binds through its polypeptide moiety to the proximal ectodomain of the α-chain of LFA-1 in front of the cysteine-rich region of the CD18 and then modifies the access to the ion binding sites or ligand-induced binding sites through its single GAG chain.

The proteoglycan ESM-1, which is secreted by endothelial cells, interacts with LFA-1 and may directly influence LFA-1 function. Thus, ESM-1 may be implicated in the regulation of leukocyte extravasation at the inflammatory sites, because of the essential role of the ICAM-1/LFA-1 interactions during firm adhesion of human lymphocytes and monocytes. In addition, ESM-1 might modulate the LFA-1/ICAM-1 costimulatory pathway on T cells and might orientate the Th1/Th2 balance of the immune response, as it has been reported for anti-ICAM-1 and anti-LFA-1 blocking mAbs (35–37). It is of note that ESM-1 circulates in plasma from healthy subjects and is increased in acute and severe inflammation (20), suggesting that ESM-1 may exert its effects in both healthy and pathological contexts. As ESM-1 levels in blood can reach $>$100 ng/ml in patients with septic shock (our unpublished data), which are concentrations close to those used here in vitro, it can be speculated that ESM-1 may have potent in vivo regulatory activity on ICAM-1- and LFA-1-mediated functions. Thus, ESM-1 may be considered as a novel class of natural endothelial cell-derived molecules able to regulate LFA-1-ICAM-1 interactions and probably LFA-1-mediated functions. It also offers new insights in the context of drug design in anti-inflammation strategy.

Acknowledgments

We thank Gwenola Kervoaze and Genevieve Marchandise for their precious technical help.

References

1. Springer, T. A. 1990. Adhesion receptors of the immune system. *Nature 346:425.*
2. Springer, T. A. 1994. Traffic signals for lymphocyte recirculation and leukocyte emigration: the multistep paradigm. *Cell 76:301.*
3. Hynes, R. O. 1992. Integrins: versatility, modulation, and signaling in cell adhesion. *Cell 69:11.*
4. Diamond, M. S., and T. A. Springer. 1994. The dynamic regulation of integrin adhesiveness. *Curr. Biol. 4:506.*
5. Shaw, A. S., and M. L. Dustin. 1997. Making the T cell receptor go the distance: a topological view of T cell activation. *Immunity 6:361.*
6. Hogg, N., and R. C. Landis. 1993. Adhesion molecules in cell interactions. *Curr. Opin. Immunol. 5:383.*
7. Jenks, S. A., and J. Miller. 2000. Inhibition of IL-4 responses after T cell priming in the context of LFA-1 costimulation is not reversed by restimulation in the presence of CD28 costimulation. *J. Immunol. 164:72.*
8. Wulfing, C., M. D. Sjaastad, and M. M. Davis. 1998. Visualizing the dynamics of T cell activation: intracellular adhesion molecule 1 migrates rapidly to the T cell/B cell interface and acts to sustain calcium levels. *Proc. Natl. Acad. Sci. USA 95:6302.*
9. Guerette, B., D. Skuk, F. Celestin, C. Huard, F. Tardif, I. Asselin, B. Roy, M. Goulet, R. Roy, M. Entman, and J. P. Tremblay. 1997. Prevention by anti-LFA-1 of acute myoblast death following transplantation. *J. Immunol. 159:2522.*
10. Tajra, L. C., X. Martin, J. Margonari, N. Blanc-Brunat, M. Ishibashi, G. Vivier, G. Panaye, J. P. Steghens, H. Kawashima, M. Miyasaka, et al. 1999. In vivo effects of monoclonal antibodies against rat β_2 integrins on kidney ischemia-reperfusion injury. *J. Surg. Res. 87:32.*
11. Arai, K., M. Sunamura, Y. Wada, M. Takahashi, M. Kobari, K. Kato, H. Yagita, K. Okumura, and S. Matsuno. 1999. Preventing effect of anti-ICAM-1 and anti-LFA-1 monoclonal antibodies on murine islet allograft rejection. *Int. J. Pancreatol. 26:23.*
12. Suzuki, J., M. Isobe, A. Izawa, W. Takahashi, S. Yamazaki, Y. Okubo, J. Amano, and M. Sekiguchi. 1999. Differential Th1 and Th2 cell regulation of murine cardiac allograft acceptance by blocking cell adhesion of ICAM-1/LFA-1 and VCAM-1/VLA-4. *Transpl. Immunol. 7:65.*
13. Isobe, M., J. Suzuki, S. Yamazaki, Y. Yazaki, S. Horie, Y. Okubo, K. Maemura, and M. Sekiguchi. 1997. Regulation by differential development of Th1 and Th2 cells in peripheral tolerance to cardiac allograft induced by blocking ICAM-1/LFA-1 adhesion. *Circulation 96:2247.*
14. Landis, R. C., A. McDowall, C. L. Holness, A. J. Littler, D. L. Simmons, and N. Hogg. 1994. Involvement of the "I" domain of LFA-1 in selective binding to ligands ICAM-1 and ICAM-3. *J. Cell Biol. 126:529.*
15. Muchowski, P. J., L. Zhang, E. R. Chang, H. R. Soule, E. F. Plow, and M. Moyle. 1994. Functional interaction between the integrin antagonist neutrophil inhibitory factor and the I domain of CD11b/CD18. [Published erratum appears in *1995 J. Biol. Chem. 270:6420.*] *J. Biol. Chem. 269:26419.*
16. Diamond, M. S., and T. A. Springer. 1993. A subpopulation of Mac-1 (CD11b/CD18) molecules mediates neutrophil adhesion to ICAM-1 and fibrinogen. *J. Cell Biol. 120:545.*
17. Kern, F., W. D. Docke, P. Reinke, and H. D. Volk. 1994. Discordant expression of LFA-1, VLA-4α, VLA-β1, CD45RO and CD28 on T-cell subsets: evidence for multiple subsets of "memory" T cells. *Int. Arch. Allergy Immunol. 104:17.*
18. Madden, K., J. Janczak, G. McEnroe, D. Lim, T. Hartman, D. Liu, and L. Stanton. 1997. A peptide derived from neutrophil inhibitory factor (NIF) blocks neutrophil adherence to endothelial cells. *Inflamm. Res. 46:216.*

Downloaded from http://www.jimmunol.org/ by guest on March 21, 2019

19. Lassalle, P., S. Molet, A. Janin, J. V. Heyden, J. Tavernier, W. Fiers, R. Devos, and A. B. Tonnel. 1996. ESM-1 is a novel human endothelial cell-specific molecule expressed in lung and regulated by cytokines. *J. Biol. Chem. 271:20458.*
20. Bechard, D., V. Meignin, A. Scherpereel, S. Oudin, G. Kervoaze, P. Bertheau, A. Janin, A. B. Tonnel, and P. Lassalle. 2000. Characterization of the secreted form of endothelial-cell-specific molecule 1 by specific monoclonal antibodies. *J. Vasc. Res. 37:417.*
21. Matsumoto, G., M. P. Nghiem, N. Nozaki, R. Schmits, and J. M. Penninger. 1998. Cooperation between CD44 and LFA-1/CD11a adhesion receptors in lymphokine-activated killer cell cytotoxicity. *J. Immunol. 160:5781.*
22. Woska, J. R., Jr., M. M. Morelock, D. D. Jeanfavre, G. O. Caviness, B. J. Bormann, and R. Rothlein. 1998. Molecular comparison of soluble intercellular adhesion molecule (sICAM)- 1 and sICAM-3 binding to lymphocyte function-associated antigen-1. *J. Biol. Chem. 273:4725.*
23. Griggs, D. W., C. M. Schmidt, and C. P. Carron. 1998. Characteristics of cation binding to the I domains of LFA-1 and MAC-1: the LFA-1 I domain contains a Ca^{2+}-binding site. *J. Biol. Chem. 273:22113.*
24. Huang, C., C. Lu, and T. A. Springer. 1997. Folding of the conserved domain but not of flanking regions in the integrin β_2 subunit requires association with the α subunit. *Proc. Natl. Acad. Sci. USA 94:3156.*
25. Stephens, P., J. T. Romer, M. Spitali, A. Shock, S. Ortlepp, C. G. Figdor, and M. K. Robinson. 1995. KIM127, an antibody that promotes adhesion, maps to a region of CD18 that includes cysteine-rich repeats. *Cell Adhes. Commun. 3:375.*
26. Dustin, M. L., and T. A. Springer. 1989. T-cell receptor cross-linking transiently stimulates adhesiveness through LFA-1. *Nature 341:619.*
27. Iida, J., A. M. Meijne, T. R. Oegema, Jr., T. A. Yednock, N. L. Kovach, L. T. Furcht, and J. B. McCarthy. 1998. A role of chondroitin sulfate glycosaminoglycan binding site in $\alpha_4\beta_1$ integrin-mediated melanoma cell adhesion. *J. Biol. Chem. 273:5955.*
28. Dransfield, I., C. Cabanas, A. Craig, and N. Hogg. 1992. Divalent cation regulation of the function of the leukocyte integrin LFA-1. *J. Cell Biol. 116:219.*
29. Graham, I. L., and E. J. Brown. 1991. Extracellular calcium results in a conformational change in Mac-1 (CD11b/CD18) on neutrophils: differentiation of adhesion and phagocytosis functions of Mac-1. *J. Immunol. 146:685.*
30. Jackson, A. M., A. B. Alexandroff, M. B. Lappin, K. Esuvaranathan, K. James, and G. D. Chisholm. 1994. Control of leucocyte function-associated antigen-1-dependent cellular conjugation by divalent cations. *Immunology 81:120.*
31. Shimizu, Y., and J. L. Mobley. 1993. Distinct divalent cation requirements for integrin-mediated $CD4^+$ T lymphocyte adhesion to ICAM-1, fibronectin, VCAM-1, and invasin. *J. Immunol. 151:4106.*
32. Altieri, D. C. 1991. Occupancy of CD11b/CD18 (Mac-1) divalent ion binding site(s) induces leukocyte adhesion. *J. Immunol. 147:1891.*
33. Hogg, N., R. Bennett, C. Cabanas, and I. Dransfield. 1992. Leukocyte integrin activation. *Kidney Int. 41:613.*
34. Binnerts, M. E., and Y. van Kooyk. 1999. How LFA-1 binds to different ligands. *Immunol. Today 20:240.*
35. Salomon, B., and J. A. Bluestone. 1998. LFA-1 interaction with ICAM-1 and ICAM-2 regulates Th2 cytokine production. *J. Immunol. 161:5138.*
36. Takamoto, M., M. Isobe, and K. Sugane. 1998. The role of ICAM-1/LFA-1 and VCAM-1/VLA-4 interactions on T helper 2 cytokine production by lung T cells of *Toxocara canis*-infected mice. *Immunology 95:419.*
37. Zuckerman, L. A., L. Pullen, and J. Miller. 1998. Functional consequences of costimulation by ICAM-1 on IL-2 gene expression and T cell activation. *J. Immunol. 160:3259.*

Downloaded from http://www.jimmunol.org/ by guest on March 21, 2019